

Accepted Manuscript

Title: Effect of Cu and Sn promotion on the catalytic deoxygenation of model and algal lipids to fuel-like hydrocarbons over supported Ni catalysts

Author: Ryan Loe Eduardo Santillan-Jimenez Tonya Morgan
Lilia Sewell Yaying Ji Samantha Jones Mark A. Isaacs Adam
F. Lee Mark Crocker

PII: S0926-3373(16)30198-9
DOI: <http://dx.doi.org/doi:10.1016/j.apcatb.2016.03.025>
Reference: APCATB 14635

To appear in: *Applied Catalysis B: Environmental*

Received date: 9-12-2015
Revised date: 10-3-2016
Accepted date: 12-3-2016

Please cite this article as: Ryan Loe, Eduardo Santillan-Jimenez, Tonya Morgan, Lilia Sewell, Yaying Ji, Samantha Jones, Mark A. Isaacs, Adam F. Lee, Mark Crocker, Effect of Cu and Sn promotion on the catalytic deoxygenation of model and algal lipids to fuel-like hydrocarbons over supported Ni catalysts, *Applied Catalysis B, Environmental* <http://dx.doi.org/10.1016/j.apcatb.2016.03.025>

This is a PDF file of an unedited manuscript that has been accepted for publication. As a service to our customers we are providing this early version of the manuscript. The manuscript will undergo copyediting, typesetting, and review of the resulting proof before it is published in its final form. Please note that during the production process errors may be discovered which could affect the content, and all legal disclaimers that apply to the journal pertain.

Effect of Cu and Sn promotion on the catalytic deoxygenation of model and algal lipids to fuel-like hydrocarbons over supported Ni catalysts

Ryan Loe^{1,2}, Eduardo Santillan-Jimenez¹, Tonya Morgan¹, Lilia Sewell¹, Yaying Ji¹, Samantha Jones^{1,2}, Mark A. Isaacs³, Adam F. Lee³, Mark Crocker^{1,2*}

¹Center for Applied Energy Research, University of Kentucky, 2540 Research Park Drive, Lexington, KY 40511, USA

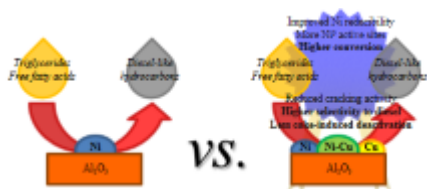
²Department of Chemistry, University of Kentucky, Lexington, KY 40506, USA

³European Bioenergy Research Institute, Aston University, Aston Triangle, Birmingham B4 7ET, United Kingdom

*Corresponding author: Tel.: +1 859 257 0295; Fax: +1 859 257 0220

e-mail: mark.crocker@uky.edu

Graphical Abstract



Highlights

- Supported Ni catalysts used to convert lipids to diesel were promoted with Cu or Sn
- Addition of 5% Cu to 20%Ni/Al₂O₃ resulted in pronounced promotion effects
- Cu improved Ni reducibility, leading to more active Ni⁰ sites and higher conversion
- Cu curbed cracking, leading to higher selectivity to diesel and reduced deactivation
- Cu promotion was observed in semi-batch and continuous runs involving various lipids

Abstract

The ability of Cu and Sn to promote the performance of a 20% Ni/Al₂O₃ catalyst in the deoxygenation of lipids to fuel-like hydrocarbons was investigated using model triglyceride and fatty acid feeds, as well as algal lipids. In the semi-batch deoxygenation of tristearin at 260 °C a pronounced promotional effect was observed, a 20% Ni-5% Cu/Al₂O₃ catalyst affording both higher conversion (97%) and selectivity to C10-C17 alkanes (99%) in comparison with unpromoted 20% Ni/Al₂O₃ (27% conversion and 87% selectivity to C10-C17). In the same reaction at 350 °C, a 20% Ni-1% Sn/Al₂O₃ catalyst afforded the best results, giving yields of C10-C17 and C17 of 97% and 55%, respectively, which contrasts with the corresponding values of 87 and 21% obtained over 20% Ni/Al₂O₃. Equally encouraging results were obtained in the semi-batch deoxygenation of stearic acid at 300 °C, in which the 20% Ni-5% Cu/Al₂O₃ catalyst afforded the highest yields of C10-C17 and C17. Experiments were also conducted at 260 °C in a fixed bed reactor using triolein – a model unsaturated triglyceride – as the feed. While both 20% Ni/Al₂O₃ and 20% Ni-5% Cu/Al₂O₃ achieved quantitative yields of diesel-like hydrocarbons at all reaction times sampled, the Cu-promoted catalyst exhibited higher selectivity to longer chain

hydrocarbons, a phenomenon which was also observed in experiments involving algal lipids as the feed. Characterization of fresh and spent catalysts indicates that Cu enhances the reducibility of Ni and suppresses both cracking reactions and coke-induced deactivation.

Keywords: Nickel; Copper; Tin; Deoxygenation; Lipids

1. Introduction

The non-renewable nature of fossil fuels and the environmental impacts of the CO₂ emissions resulting from their combustion demand the development of alternative fuels that are both sustainable and carbon neutral. Biofuels fulfill these two conditions, as they derive from a renewable resource – biomass – and they have the potential for closing the carbon cycle without disrupting the food supply when produced from waste and nonedible biomass feedstocks [1-3]. The production of biodiesel – a biofuel consisting of fatty acid methyl esters (FAMES) – via the transesterification of vegetable oils or animal fats offers one pathway for the production of renewable liquid fuels. Biodiesel has certain advantages compared to traditional petroleum-derived fuels, such as high cetane number and increased lubricity [4]. However, the high oxygen content of FAMES gives rise to several drawbacks including poor storage stability and cold flow properties. Therefore, interest has shifted to the development of catalytic methods for the deoxygenation of triglyceride and fatty acid feeds to fuel-like hydrocarbons [4, 5].

Hydrodeoxygenation (HDO) and decarboxylation/decarbonylation (deCO_x) represent two processes that have been developed to remove the oxygen from fats and oils in the form of H₂O and CO₂/CO, respectively [6, 7]. Although effective, HDO requires high H₂ pressures and the use of sulfided catalysts, both of which are problematic. Indeed, the H₂ pressures required for HDO limit the process to centralized facilities and the sulfided catalysts risk contaminating the products with sulfur and tend to deactivate in the presence of water, a co-product of the HDO reaction [8, 9]. In contrast, deCO_x proceeds under lower H₂ pressures and does not require the use of sulfided catalysts.

Much of the previous work concerning deCO_x has focused on supported Pd [7, 10-18] or Pt [19-21] catalysts, which exhibit high conversion and selectivity to diesel-like hydrocarbons. However, the high cost of these precious metals can forestall their use in large industrial

applications. Significantly, inexpensive Ni-based catalysts have exhibited near comparable results to Pd- and Pt-based formulations in converting lipid-based feeds to fuel-like hydrocarbons [22, 23], the Ni-catalyzed transformation of triglycerides and related compounds to green diesel being the subject of a recent review by Kordulis et al. [24]. The fact that good conversions and selectivities have been achieved on Ni catalysts incorporating metal oxide supports – as opposed to high surface area carbon supports – is particularly noteworthy [25-27]. Indeed, carbon-supported catalysts typically lead to better yields in deCO_x reactions due to the more favorable adsorption of fatty acids on the catalyst [28]; however, deCO_x catalysts are susceptible to deactivation by the accumulation of carbonaceous deposits on their surface [13, 15, 16, 29-32], which makes metal oxide supports advantageous since they allow for spent catalyst to be easily regenerated by simply combusting these deposits [33].

Although oxide supported Ni catalysts have shown promising activity in deCO_x reactions, they require further improvement if they are to become viable candidates for the production of fuel-like hydrocarbons. Specifically, Ni catalysts have a tendency to produce light hydrocarbons and thus, improving the selectivity towards the longer chain products that constitute diesel fuel (~C10-C20 hydrocarbons [34]) is desirable. As mentioned above, catalyst deactivation is also an issue for deCO_x catalysts, Ni-based formulations being particularly prone to coking [35]. It can be postulated that these issues are both related to the high activity of Ni for C-C cracking, given that cracking reactions result in the formation of light products and cause the accumulation of organic material on the catalyst, leading to its deactivation. This problem has been addressed in other Ni-catalyzed reactions by the addition of promoters such as Cu and Sn. Compared to monometallic Ni catalysts, supported catalysts containing a Ni-Cu alloy phase have shown superior performance in methane dissociation [36], ethanol reforming [37], ethylene hydrogenation reactions [38] and the hydrodeoxygenation of algae-derived pyrolysis oil [39]. One explanation for this improved performance is that nickel carbide phases can readily form on monometallic Ni catalysts, which leads to the formation of graphitic carbon deposits on the active sites of the catalyst. Since Cu does not form a carbide phase, Ni-Cu catalysts are less prone to coking than their monometallic analogs [37, 40]. Evidence suggests that the formation of carbon deposits on Ni particles occurs at step edges and that these are the sites preferentially occupied by Cu, which explains why Cu-doped Ni catalysts are less prone to deactivation [36].

Also of note in this context is a report by Yakovlev et al. concerning the HDO of anisole and FAMEs, in which Ni-Cu catalysts were found to outperform their monometallic Ni counterparts [41]. The authors of this study attributed the superior performance of the bimetallic catalysts to the ability of copper to simultaneously facilitate nickel oxide reduction and prevent the methanation of oxygen-containing molecules.

Bimetallic catalysts comprising Sn as a Ni promoter have also been shown to outperform Ni-only catalysts in steam reforming [42, 43]. As with Ni-Cu catalysts, the improvement in activity has been attributed to the decrease in coke formation resulting from Sn doping. Indeed, it has been reported that Sn can lower the binding energy of carbon on the Ni surface sites that serve as nucleation centers for the carbon deposits [42], which has the potential to decrease the catalyst deactivation caused by coking. Similar to the case of Ni-Cu catalysts, the promoting effect of Sn can likewise be explained on the basis of metal particle morphology, since Sn atoms can occupy step edge sites which are otherwise the Ni sites most responsible for coking [43].

Based on the foregoing, the effect of promoting Ni with Cu or Sn in the deCO_x of tristearin and stearic acid – used respectively as model triglyceride and fatty acid compounds – was studied in the present work. Initially, reaction temperature and the level of doping were systematically changed in semi-batch experiments to find the optimum set of conditions. The best Ni-promoter combination was then tested in a fixed bed reactor to evaluate the bimetallic catalyst in continuous mode and obtain results more relevant to industrial applications. In fixed bed reactions triolein – a triglyceride with a double bond between the 9th and 10th carbons in each acyl chain – was used as a model unsaturated triglyceride feed. Given that unsaturated feeds are more prone to cracking than saturated feeds [44], thereby exacerbating catalyst deactivation, the use of triolein represents a good test of the ability of promoters to improve both selectivity to long chain hydrocarbons and catalyst resistance to deactivation.

2. Experimental

2.1. Catalyst preparation and characterization

Catalysts were prepared by excess wetness impregnation using, as appropriate, Ni(NO₃)₂ • 6H₂O (Alfa Aesar), Cu(NO₃)₂ • 3H₂O (Sigma Aldrich), and SnCl₂ • 2H₂O (Gelest, Inc.) as the metal precursors and γ -Al₂O₃ (Sasol; surface area of 216 m²/g) as the support. Ni loading was

kept constant at 20 wt.%, while the Cu or Sn loading was varied. The impregnated materials were dried overnight at 60 °C under vacuum before calcination at 500 °C for 3 h in static air.

The surface area, pore volume and average pore radius of the catalysts were determined by N₂ physisorption using previously described instruments and methods [22]. The average NiO particle size was found by applying the Scherrer equation to the NiO peaks observed in powder X-ray diffractograms, which were acquired using equipment and procedures described previously [25]. Thermogravimetric analysis (TGA) of the spent catalysts was performed under flowing air (50 mL/min) on a TA instruments Discovery Series thermogravimetric analyzer. The temperature was ramped from room temperature to 800 °C at a rate of 10 °C/min. Temperature-programmed reduction (TPR) was used to study the reducibility of the catalysts employing instrumentation and methods described in a previous contribution [25]. For pulsed H₂ chemisorption measurements, the catalyst (250 mg) was first reduced under 10% H₂/Ar flow at 350 °C for 1 h. The U-tube reactor was then purged with Ar at 450 °C for 30 min, and then cooled under flowing Ar to 45 °C. 0.025 mL (STP) 10% H₂/Ar was then pulsed into the Ar carrier gas flowing to the reactor (at 50 mL/min). Pulsing was continued at 3 min intervals until the area of the H₂ peaks remained constant.

X-ray photoelectron spectroscopy (XPS) was undertaken on a Kratos AXIS HSi spectrometer equipped with a charge neutralizer and monochromated Al K_α excitation source (1486.7 eV), with energies referenced to adventitious carbon at 284.6 eV. High resolution spectra were acquired with a pass energy of 40 eV. Spectral fitting was performed using CasaXPS version 2.3.14, utilizing a common Gaussian-Lorentzian lineshape and FWHM for each element, and the relevant instrumental response factors for quantification. The minimum number of components required to minimize the residual difference between experiment data and fitting model was employed in all cases.

Diffuse reflectance infrared Fourier transform spectroscopy (DRIFTS) was performed on the 20% Ni/Al₂O₃ and the 20% Ni-5% Cu/Al₂O₃ catalysts during CO adsorption. The catalysts were reduced *in situ* in 10% H₂/N₂ flow (120 mL/min) at 350 °C for 1 h. The reactor was then purged with Ar while the temperature was raised to 450 °C (hold time 30 min) to remove adsorbed hydrogen prior to cooling the catalyst to 50 °C under flowing Ar. Each CO adsorption measurement was performed with 10% CO/He at 50 °C for 30 min, followed by Ar purging to

remove gas phase CO and weakly adsorbed CO. Spectra were collected every 30 s during Ar purging until there was no change in IR band intensity.

Materials for electron microscopy were supported on Au grids purchased from Electron Microscopy Sciences. Transmission electron microscopy (TEM) and scanning transmission electron microscopy (STEM) studies were conducted using a field emission JEOL 2010F with a URP pole piece, GATAN 200 GIF, GATAN DigiScann II, Fischione HAADF STEM detector, Oxford energy-dispersive X-ray detector and EmiSpec EsVision software. STEM measurements were acquired for both samples using a high-resolution probe at 2 Å.

2.2. Deoxygenation experiments in semi-batch mode

Tristearin (95%, obtained from City Chemical) and stearic acid (97%, obtained from Acros Organics) were respectively used as model saturated triglyceride and fatty acid compounds. Details on the acid number and the distribution of fatty acids in the tristearin employed are available elsewhere [33]. Experiments were performed in a 100 mL stainless steel, mechanically stirred autoclave. The catalyst (0.5 g) was added in powder form (<150 µm particle size) to the reactor, which was then purged with argon. The catalyst was subsequently reduced at 350 °C under a flow (~60 mL/min) of 10% H₂/N₂ for 3 h prior to cooling to room temperature, purging the reactor with Ar, and adding both solvent and feed (in experiments involving tristearin 22 g of dodecane and 1.8 g of feed was used while in experiments involving stearic acid 28.8 g of solvent and 1.72 g of feed was employed). After the addition of feed and solvent, the autoclave was purged three times with Ar prior to being pressurized with H₂ (to 580 psi and 300 psi for experiments involving tristearin and stearic acid, respectively) and heated to the reaction temperature, which was measured by a K-type thermocouple placed inside a thermowell. A constant flow of 60 mL/min of H₂ and mechanical stirring of 1,000 rpm was maintained during each experiment. Volatile products were collected from the gas stream exiting the reactor by a condenser kept at room temperature. At the end of these reactions, which lasted 6 and 1.5 h when tristearin and stearic acid were employed, respectively, forced air and an ice bath were used to cool the reactor to room temperature while the system was slowly depressurized. The liquid product mixture and the spent catalyst were removed from the reactor and separated by gravity filtration, the catalyst being washed twice with chloroform to yield

additional material. All experiments for which results are shown were performed a minimum of two times.

2.3. Deoxygenation experiments in continuous mode

Triolein (glyceryl trioleate, $\geq 99\%$) was purchased from Sigma-Aldrich, details on the acid number and the distribution of fatty acids in the triolein being reported elsewhere [45]. Algal lipids were extracted via the Bligh-Dyer method [46] from a sample of dry *Scenedesmus* sp. grown in a photobioreactor fed with the flue gas of a coal-fired power plant [47]. Extracted lipids were then purified using a column containing both activated carbon (DARCO® KB-G purchased from Sigma-Aldrich) and silica gel. Experimental details on algae culturing as well as algal lipids extraction and purification can be found in a recent contribution [47]. Deoxygenation experiments in continuous mode were performed in a fixed bed stainless steel tubular reactor (1/2 in o.d.) equipped with an HPLC pump. The catalyst (0.5 g, particle size 150-300 μm , held in place using a stainless steel frit) was reduced under flowing H_2 at 400 $^\circ\text{C}$ for 3 h. Next, the system was taken to the reaction temperature (260 $^\circ\text{C}$) and pressurized with H_2 to 580 psi. A liquid solution of the feed in dodecane (1.33 wt% triolein) was introduced to the system at a rate of 0.2 mL/min along with a flow of H_2 (50 mL/min). A liquid gas separator (kept at 0 $^\circ\text{C}$) placed downstream from the catalyst bed was used to collect liquid samples.

2.4. Product analysis

All feeds and reaction products were analyzed using a GC method specifically devised to identify and quantify the constituents of the feeds used and the products obtained in the upgrading of fats and oils to hydrocarbons, detailed information about the development and application of this method being available elsewhere [48]. Briefly, analyses were performed using an Agilent 7890A GC equipped with an Agilent Multimode inlet, a deactivated open ended helix liner and a flame ionization detector (FID). Helium was used as the carrier gas and a 1 μL injection was employed. The FID was set to 350 $^\circ\text{C}$ with the following gas flow rates: $\text{H}_2=30$ mL/min; air=400 mL/min; makeup= 5mL/min. The inlet was ran in split mode (split ratio 25:1; split flow 50 mL/min) using an initial temperature of 100 $^\circ\text{C}$. Inlet temperature was increased immediately upon injection (at a rate of 8 $^\circ\text{C}/\text{min}$) to a final temperature of 320 $^\circ\text{C}$, which was maintained for the duration of the analysis. The initial oven temperature of 45 $^\circ\text{C}$ was

immediately increased upon injection first to 325 °C (at a rate of 4 °C/min) and then to 400 °C (at a rate of 10 °C/min). This temperature was then maintained for 12.5 minutes, making the total run time 90 minutes. An Agilent J&W DB-5HT column (30 m × 250 µm × 0.1 µm) rated to 400 °C was employed along with a constant He flow of 2 mL/min. Quantification was performed using cyclohexanone as internal standard. Agilent Chemstation and Separation Systems Inc. SimDis Expert 9 software were respectively used to perform chromatographic programming and to process the chromatographic data acquired. Solvents (i.e., chloroform and dodecane) and internal standard (cyclohexanone) were quenched and/or subtracted prior to processing the data, which precluded the acquisition of quantitative data for linear C5-C9 hydrocarbons.

3. Results and Discussion

3.1. Catalyst Characterization

The X-ray diffractograms in Figure S1 in the supplementary material show that all catalysts present diffraction peaks – at 37.2°, 43.3°, 62.9°, 75.4° and 79.4° – indicative of NiO [49]. Notably, peaks at 35.5° and 38.7° corresponding to a distinct CuO phase [50] are not observed, which may be the result of the low amount of Cu; indeed, several authors have reported that these peaks are not discernable at low Cu loadings [49, 51]. However, all of the NiO peaks increase in intensity as the Cu metal loading increases. This is consistent with a report by Lee et al., who observed that an increase in the amount of Cu in Ni-Cu/Al₂O₃ catalysts results in an increase in XRD peak intensity and in the formation of Ni-Cu mixed oxides [51].

The textural properties and the average NiO particle size of the catalysts used in this study are collected in Table 1. The effect of promoter addition on the average particle size of NiO was studied by applying the Scherrer equation to the X-ray diffractograms of the promoted catalysts. Evidently, at low loadings, the addition of the promoter does not have a direct impact on the NiO particle size, as illustrated by the fact that 20% Ni-2% Cu/Al₂O₃ had the smallest NiO particle size (6.4 nm) of all the catalysts. However, the NiO particle size in the 20% Ni-5% Cu/Al₂O₃ sample (10.7 nm) was the largest among the samples, which points to an increase of particle size at high Cu loadings. TEM and STEM imaging of the 20% Ni/Al₂O₃ and 20% Ni-5% Cu/Al₂O₃ samples was found to be consistent with the average particle sizes reported in Table 1,

STEM-EDX revealing the presence of Ni-Cu, Ni-only and Cu-only particles in 20% Ni-5% Cu/Al₂O₃ (see Figures S2 and S3 in the supplementary material). This agrees with TPR data (vide infra), in which the bimetallic catalysts show separate reduction maxima corresponding to particles of these compositions.

The TPR profiles of the catalysts, which are shown in Figure 1, indicate that an increase in Cu loading results in a decrease in the reduction temperature of the catalyst. The 20% Ni/Al₂O₃ catalyst shows a broad reduction peak, which can be attributed to the reduction of NiO to metallic Ni, with a maximum at 507 °C [52]; however, a small shoulder showing a local maximum at 300 °C (assigned to the reduction of large Ni ensembles [52]) can also be seen. The main reduction event also shows an indistinct shoulder above 700 °C that can be assigned to the reduction of a NiAl₂O₄ phase, a feature more clearly displayed by the other catalysts examined (vide infra). The TPR profile of 20% Ni-1% Cu/Al₂O₃ shows two similar reduction events, a broad peak with a maximum at 497 °C and a small shoulder with a maximum at 275 °C, these peaks sharing the aforementioned assignments and the shift of their maxima to lower temperature being attributable to the presence of Cu [53]. In addition, the main peak is accompanied by two shoulders, one centered around 385 °C, which can be attributed to the reduction of a NiO-CuO phase [54] and one centered around 710 °C which can be assigned to nickel aluminate (NiAl₂O₄) formed from the reaction of NiO with the Al₂O₃ support [55]. Notably, the TPR profile for 20% Ni-2% Cu/Al₂O₃ displays five distinct reduction events: 1) a peak with a maximum at 480 °C attributable to the reduction of NiO to Ni metal; 2) a shoulder of the latter peak, centered around 700 °C, which is assigned to the reduction of NiAl₂O₄; 3) a main peak with a maximum at 355 °C attributed to the reduction of a NiO-CuO phase ; 4) a shoulder of this peak centered around 255 °C signaling the reduction of large NiO and/or NiO-CuO ensembles; and 5) a small but well-defined peak with a maximum at 200 °C due to the reduction of copper oxides to Cu metal [49, 53]. This last assignment was confirmed by TPR measurement of a 5% Cu/Al₂O₃ sample (not shown). In line with the aforementioned trends, the TPR profile for 20% Ni-5% Cu/Al₂O₃ also shows several reduction events, including broad peaks centered around 688 °C and 453 °C (due to the reduction of NiAl₂O₄ and NiO, respectively), and well-defined peaks with maxima at 355 °C and 180 °C, attributed to the reduction of a NiO-CuO phase and to that of copper oxides, respectively. In short, Cu addition reduces the reduction

temperature of NiO in agreement with observations recently reported by Guo et al. [39]. Moreover, the reduction temperature of both nickel and copper oxides decreases as the Cu loading increases, a phenomenon that has also been observed by other authors [53]. In turn, the decrease in the reduction temperature of Ni resulting from Cu addition leads to the creation of additional Ni⁰; XPS of reduced 20%Ni/Al₂O₃ and 20%Ni-5%Cu/Al₂O₃ confirming that the bimetallic catalyst has more than double the concentration of Ni⁰ at the catalyst surface (see Figure S4 in the supplementary material). This explains in part the improved performance that certain Ni-Cu catalysts display relative to the Ni-only sample (see sections 3.3-3.6), since Ni⁰ is believed to be the catalytically active phase for lipid deoxygenation.

Figure 1 also shows the TPR profile for 20% Ni-1% Sn/Al₂O₃, which shows a main peak with a maximum at 500 °C and a shoulder centered around 700 °C, along with a small but well-defined peak with a maximum at 307 °C. The effect of Sn on the TPR profiles seems to be limited to a narrowing of the peaks displayed by the Ni-only catalyst, which is in line with a previous report by Castaño et al., who concluded that metals with a lower surface tension and larger atomic radius than Ni do not form alloys with the latter since they are expelled from the matrix and segregate strongly [56].

H₂ chemisorption was performed on the 20% Ni/Al₂O₃ and the 20% Ni-5% Cu/Al₂O₃ catalysts in order to evaluate the amount of metal active sites present on the catalyst surface after reduction at 350 °C (corresponding to the catalyst reduction temperature applied in the semi-batch experiments). The monometallic and bimetallic catalysts exhibited a H₂ uptake of 0.1569 and 0.4943 mL/g, respectively, corresponding to roughly 8.433x10¹⁸ and 2.658x10¹⁹ reduced surface metal sites per gram of catalyst. The larger volume of H₂ adsorbed at this temperature is consistent with the lower reduction temperature of the metals in the bimetallic catalysts as observed in the TPR measurements and is in good quantitative agreement with the surface Ni⁰ content determined directly by XPS.

DRIFTS measurements made on the 20% Ni-5% Cu/Al₂O₃ sample after CO adsorption further confirmed the presence of an electronic interaction between Ni and Cu. As shown in Figure S5 in the supplementary material, when the monometallic Ni catalyst was reduced at 350 °C and CO was subsequently adsorbed at room temperature, band intensity in the CO stretching

region was extremely weak. However, when the reduction temperature was increased to 500 °C, two CO adsorption bands were observed. A band at 2036 cm⁻¹ can be assigned to CO linearly adsorbed on Ni⁰, while a low frequency band at 1960 cm⁻¹ can be assigned to CO bridge-bonded to Ni⁰ [53]. For the bimetallic Ni-Cu catalyst, significant Ni reduction took place at 350 °C, as evidenced by the presence of strong CO bands. Notably, the CO bands observed at 2036 and 1960 cm⁻¹ by 20% Ni/Al₂O₃ after reduction at 500 °C showed a red shift – indicative of an electronic interaction between Ni and Cu – to 2010 and 1890 cm⁻¹ in 20% Ni-5% Cu/Al₂O₃ reduced at 350 °C, the first CO band showing a concomitant increase in intensity, implying that the formation of additional Ni⁰ sites was facilitated by the presence of Cu [53, 57, 58]. An additional band at 2121 cm⁻¹ can be attributed to CO adsorbed on Cu sites [53, 59, 60], which is in agreement with the fact that an intense band was observed in the same position for a 5% Cu/Al₂O₃ reference sample. Other bands (1660, 1435 and 1228 cm⁻¹) can be assigned to bicarbonate formed on the Al₂O₃ support [61]. XPS further evidences electron transfer between Ni and Cu, with the introduction of copper shifting the Ni 2p_{3/2} XP peak to lower binding energy (Figure S6), from 854.5 eV in 20% Ni/Al₂O₃ to 853.4 eV in 20% Ni-5% Cu/Al₂O₃, consistent with enhanced nickel reduction.

3.2. Blank runs

The results obtained when tristearin and stearic acid are submitted to the reaction conditions described in section 2.2 in the absence of a catalyst have been previously reported and discussed [23]. In short, stearic acid conversion at 300 °C was only 5% and selectivity to C10-C17 and C17 were approximately 85% and 15%, respectively. For blank experiments using tristearin at 360 °C, conversion was around 85% and selectivity to C10-C17 and C17 were ca. 47% and 14%, respectively. These observations are in agreement with thermal (non-catalytic) experiments by other workers [62, 63], the differing reactivity of stearic acid and tristearin being attributed to the more forcing conditions employed with the latter. Notably, an additional blank experiment was performed by subjecting dodecane to tristearin deoxygenation conditions in the presence of a supported Ni catalyst; dodecane proved entirely unreactive and hence, none of the reaction products detected in the experiments described below arose from the reaction solvent.

3.3. Tristearin deoxygenation in semi-batch mode

The results of tristearin deoxygenation performed at three different temperatures are summarized in Table 2. Conversion increased with increasing temperature, which is unsurprising since triglycerides are reported to thermally decompose to diglycerides, free fatty acids and hydrocarbons at temperatures approaching 360 °C [63]. Moreover, selectivity to both C10-C17 and C17 invariably decreased as the reaction temperature increased for all catalysts showing >99% tristearin conversion, as expected since higher temperatures favor cracking reactions and consequently, lighter hydrocarbons.

Remarkably, whereas the monometallic catalyst afforded only 27% conversion at 260 °C, 20% Ni-5% Cu/Al₂O₃ exhibited 97% conversion. 5% Cu/Al₂O₃ was also tested since Berenblyum et al. found this catalyst to be active in lipid deoxygenation [64, 65]; however, 5% Cu/Al₂O₃ afforded only 11% conversion at 260 °C, which indicates that the superior performance of 20% Ni-5% Cu/Al₂O₃ stems from a synergistic effect between Ni and Cu and not merely from the additive but independent contributions of these two metals. 20% Ni-1% Sn/Al₂O₃ was the worst performing of all formulations included in Table 2 at 260 °C, with only 11% conversion. Parenthetically, residual Cl (~2,400 ppm) was detected in this catalyst, which was synthesized using SnCl₂ • 2H₂O as the Sn precursor (see section 2.1). Albeit it is widely known that electronegative elements such as Cl can act as catalyst poisons by reducing electron density at the metal surface, the latter could also result in promotion effects. Indeed, it has been reported that Cl hinders coke deposition on metal nanoparticles, since a decrease in electron density at the metal surface reduces electron transfer from the metal to the π^* orbital of chemisorbed reactant molecules, thereby disfavoring their dissociative adsorption and the concurrent catalyst deactivation [66]. In addition, Cl has also been reported to increase the spillover of hydrogen from the metal to the support, which can eliminate coke precursors via hydrogenation and further reduce coke-induced deactivation [67]. Therefore, Cl may have both poisoning and promotion effects, the investigation of which is outside the scope of the present contribution.

Copper promotion was less apparent at 300 °C, a consequence of the high (98%) conversion exhibited by the monometallic Ni catalyst being similar to that of the Ni-Cu

bimetallic catalysts. The Ni-Sn catalyst again exhibited the poorest activity (38% conversion) and selectivity (45% to C10-C17 hydrocarbons), although these values were considerably improved relative to those at 260 °C. Notably, the Cu loading had little impact on the selectivity to C17 or C10-C17 hydrocarbons at 300 °C; however, at 350 °C – a temperature at which conversions invariably exceeded 99% (as expected from the results obtained at 300 °C) – it noticeably influenced selectivity. Indeed, 20% Ni-5% Cu/Al₂O₃ exhibited the highest selectivity to both C10-C17 and C17 hydrocarbons (98% and 49%, respectively), which contrasts with the 88% and 21% selectivity values obtained over the monometallic 20% Ni/Al₂O₃ catalyst. This demonstrates that doping with 5% Cu effectively curbs cracking reactions at 350 °C. Surprisingly, at 350 °C the best catalyst was 20% Ni-1% Sn/Al₂O₃, yielding 99% conversion and C10-C17 and C17 hydrocarbon selectivities of 97% and 56%, respectively. Tin promotion is thus extremely temperature dependent. It should be noted that further increasing the copper loading to 7.5% did not improve performance relative to the 20% Ni-5% Cu/Al₂O₃ catalyst.

Notably, in all experiments small amounts of reaction products with a bp higher than C17 were observed. In all cases (Table 2) product mixtures contained 1-2% of C18, which suggests that deoxygenation proceeds mainly through deCO_x rather than HDO, as also observed in experiments involving stearic acid as the feed (see section 3.4). Small amounts of fatty esters such as cetyl stearate and stearyl stearate were also observed in some product mixtures, although this was dependent on both the temperature and the catalysts employed. Indeed, at 260 °C both the Ni-only catalyst and catalysts promoted with 1% Cu or Sn afforded moderate amounts (~5%) of these esters, which were obtained in lower amounts (~2%) over 20% Ni-2% Cu/Al₂O₃ and were not observed over 20% Ni-5% Cu/Al₂O₃. At 300 °C, only the Sn-promoted catalyst yielded a small amount (~5%) of these esters, whereas at 350 °C the latter were not detected. As discussed below (section 3.4), these esters can be formed as intermediates but are completely converted to hydrocarbons in the presence of the more active catalysts.

In order to be able to unequivocally attribute improvements in catalytic performance to the presence of promoters, the effect of metal dispersion on catalyst performance must be considered to discount the possibility that the differences in Table 2 simply reflect metal particle size effects. To this end, a 20% Ni/Al₂O₃ catalyst with a markedly different average NiO particle

size of 16.1 nm was prepared (using butanol in lieu of water in the synthesis described in section 2.1) and its deoxygenation activity at 260 °C was compared to that of the 20% Ni/Al₂O₃ catalyst with an average NiO particle size of 7.4 nm, the results of these experiments being summarized in Table S1. While the catalytic properties of these two formulations differed somewhat, it is clear that the effect of copper addition cannot be explained solely in terms of its impact on NiO particle size. Indeed, increasing the particle size of the monometallic catalyst from 7.4 nm to 16.1 nm increased tristearin conversion by 11 % at the expense of a 10% decrease in selectivity to C10-C17 and a 19% decrease in selectivity to C17 (see Table S1). This contrasts with the greatly increased conversion and selectivity observed for the 20% Ni-5% Cu/Al₂O₃ at 260 °C (Table 2) relative to both 20% Ni/Al₂O₃ catalysts.

3.4. Stearic acid deoxygenation in semi-batch mode

Since triglyceride conversion to hydrocarbons via deCO_x has been reported to be intermediated by free fatty acids [22, 23, 25, 27], representative experiments were also performed using stearic acid as the feed in an effort to gain additional insights into the promoting effect of Cu and Sn. The results of these deoxygenation experiments, which were performed at two different temperatures, are shown in Table 3. Irrespective of the catalyst or temperature employed, C18 represented at most 1% of the total product yield, indicating that deoxygenation occurred principally via deCO_x (yielding C17) rather than through HDO (which would afford C18). This is consistent with previous reports indicating that deCO_x is the dominant reaction pathway over Ni-based catalysts [9, 25, 35, 68]. In line with the results obtained using tristearin, 20% Ni-5%Cu/Al₂O₃ and 20% Ni-1% Sn/Al₂O₃ respectively exhibited the highest and lowest stearic acid conversion at both temperatures. Selectivity values were more informative, since selectivities to C10-C17 hydrocarbons at 260 °C were much lower for both the Ni-only and the Ni-Cu catalysts than when tristearin was used as the feed. This is attributed to the intermediates formed during stearic acid deoxygenation. Indeed, the reaction may proceed by routes other than direct decarboxylation – as illustrated in Figure 2 – and consequently, a range of intermediates can form in accordance with previous work by the research groups of Murzin and Lercher [69, 70]. For instance, an ester (in this case stearyl stearate) can form when an alcohol intermediate

(stearyl alcohol) undergoes esterification with the stearic acid feed. In turn, the stearyl stearate thus formed requires further hydrogenation of the ester bond to form stearyl alcohol once again before the latter can form the alkane via decarbonylation. Stearyl stearate formation was indeed significant at 260 °C, yields of 13, 16, and 9% being obtained after 1.5 h over 20% Ni/Al₂O₃, 20% Ni-5% Cu/Al₂O₃, and 20% Ni-1% Sn/Al₂O₃, respectively. When the reaction temperature was increased to 300 °C, the yield of C10-C17 hydrocarbons surged while that of stearyl stearate decreased to 0, 4, and 7% over the Ni-only, Ni-Cu and Ni-Sn catalysts, respectively. The significant amounts of stearyl stearate intermediate detected offer a compelling explanation vis-à-vis the lower selectivity to C10-C17 hydrocarbons obtained at lower reaction temperatures. This intermediate is not observed in experiments involving tristearin as the feed, which can be attributed to the longer reaction times employed for those runs.

3.5. Triolein deoxygenation in continuous mode

Continuous processes are favored for industrial applications and hence, the effect of Cu promotion was also assessed by comparing the performance of 20% Ni/Al₂O₃ and 20% Ni-5% Cu/Al₂O₃ in a fixed bed reactor. These experiments were performed using 1.33 wt.% triolein in dodecane as the feed, triolein being chosen not only due to the fact that unsaturated lipids are commonly found in biomass-derived feeds [44], but also because in the deCO_x of lipids to hydrocarbons it has been observed that catalyst deactivation from coking occurs to a greater extent when unsaturated feeds are employed [32]; thus, triolein offers a means to gauge the ability of Cu to improve catalyst resistance to deactivation. Indeed, it has been suggested that unsaturated feeds cause catalyst deactivation due to their stronger adsorption and propensity for cracking, thus leading to coke deposition [44].

Figure 3 shows the boiling point distribution plots (BPDP) of both reactants and products from fixed bed experiments sampled at intervals of 1, 2, 3, and 4 h. These BPDPs, which were obtained through a recently published simulated distillation GC protocol [48], show that practically all products formed were hydrocarbons within the boiling range of diesel fuel (~180-350 °C) at all reaction times. Notably, heptadecane (bp = 302 °C) represented the major product in all samples, further indicating that deCO_x – as opposed to HDO – constitutes the main reaction

pathway. The superior performance of the Ni-Cu catalyst relative to the Ni-only catalyst is most prominent in the first hour of the reaction, in which long chain (C15-17) hydrocarbons comprised approximately half of the products formed over the monometallic catalyst, whereas C15-C17 constituted about three-quarters of the products afforded by the bimetallic catalyst. It is also noteworthy that while 20% Ni/Al₂O₃ showed evidence of slight deactivation after 4 h, at which time a small amount of the material appeared in the product mixture exhibiting a boiling point characteristic of the feed (600 °C) – this was not the case for 20% Ni-5% Cu/Al₂O₃. Overall, both catalysts achieved close to quantitative conversion in continuous mode at all reaction times sampled, although the bimetallic catalyst displayed higher selectivity to C15-C17 hydrocarbons (which are more desirable than light hydrocarbons since they possess higher cetane numbers) than the monometallic catalyst irrespective of time on stream.

3.6. Algal lipids deoxygenation in continuous mode

In view of the promising results obtained in the continuous deoxygenation of triolein, the upgrading of a realistic and topical feed – namely algal lipids [47] – was attempted using identical reaction conditions as those employed with triolein. The BPDP of the algae extract and the reaction products obtained over both 20% Ni/Al₂O₃ and 20% Ni-5% Cu/Al₂O₃ are included in Figure 4. As illustrated by the BPDP of the feed, compounds boiling below 320 °C (mostly hydrocarbons) represented ~7% of the algae extract, compounds boiling between 320-500 °C (mostly free fatty acids) comprised ca. 66% of the feed, and compounds boiling >500 °C (mostly triglycerides) constituted ~27% of the extract. In addition to these compounds, GC-MS of the algae extract (shown in the supplementary material as Figure S7) also revealed the presence of non-negligible amounts of other compounds such as fatty alcohols, phytols and other phytol-like compounds in agreement with a previous report [45]. Catalytic upgrading effectively increased the diesel range hydrocarbon content from ~7% in the feed to 78% and 83% at t=1 h over 20% Ni/Al₂O₃ and 20% Ni-5% Cu/Al₂O₃, respectively, the corresponding values being 42% and 45% at t=4 h. In line with a recent report [45], the lower yields of diesel-like hydrocarbons, as well as the higher rate of deactivation observed in these runs relative to experiments involving triolein as the feed, can be attributed to the fact that the algae extract contains highly unsaturated fatty acid chains, as well as compounds such as phytols, which are potentially capable of poisoning

catalytically active sites via strong adsorption. Nevertheless, the results presented herein indicate that good diesel yields can be obtained. Notably, just as for the triolein upgrading experiments, the superior performance of the Ni-Cu bimetallic catalyst relative to the Ni-only catalyst is most prominent in the first hour of the reaction, C10-C14 hydrocarbons representing ~23 and 10% of the products obtained over 20% Ni/Al₂O₃ and 20% Ni-5% Cu/Al₂O₃, respectively, once again showing that the Ni-Cu catalyst favors the formation of long chain hydrocarbons.

3.7. Spent catalyst characterization

The ability of Ni-Cu catalysts to outperform their Ni-only counterparts has been postulated to arise from decreased coking, which results in reduced catalyst deactivation and enhanced conversion [37, 40]. Representative spent catalysts were therefore subjected to thermogravimetric analysis in air to quantify surface coking, the resulting profiles being collected in Figure 5. TGA profiles show a major weight loss event below 400 °C, which could reflect either the desorption and/or combustion of residual reactants, intermediates and/or products or the combustion of poorly structured carbon deposits [33]. Notably, the weight gain centered around 350-400 °C shown by some spent catalysts in Figure 5 is due to the oxidation of Ni to NiO [71].

For some catalysts, TGA profiles showed a good correlation between the degree of coking and their conversion. For instance, in experiments performed with tristearin as the feed at 260 °C (Figure 5 top left), the spent 20% Ni-5% Cu/Al₂O₃ and 20% Ni-1% Sn/Al₂O₃ exhibited the lowest and highest weight loss, indicating the least and the greatest amount of coke formation, respectively. This is in agreement with the fact that 20% Ni-5% Cu/Al₂O₃ and 20% Ni-1% Sn/Al₂O₃ respectively showed the highest and lowest conversion. Nevertheless, all other catalysts showed almost identical weight losses, which contrasts with the fact that 20% Ni-2% Cu/Al₂O₃ displayed a considerably higher conversion than 20% Ni/Al₂O₃ and 20% Ni-1% Cu/Al₂O₃. For spent catalysts arising from experiments with tristearin as the feed at 350 °C (Figure 5 top right), all catalysts displayed a relatively small – and very similar – weight loss (7.5±1%), which is consistent with the fact that all catalysts afforded quantitative conversions.

The TGA plots of catalysts spent using stearic acid as the feed at a reaction temperature of 300 °C (Figure 5 bottom left) also illustrate that albeit in some instances there is a clear

correlation between the amount of coke deposited on catalysts and their performance (e.g., 20% Ni-5% Cu/Al₂O₃ showed the least coking and best conversion), in other cases no such correlation exists (albeit 20% Ni-1% Sn/Al₂O showed lower amounts of coke deposits than 20% Ni/Al₂O₃ the monometallic formulation afforded a substantially higher conversion). However, the weight loss difference between the Ni-only and the Ni-Sn catalysts is fairly small (~4%), which suggest that catalyst performance – and specifically the effect of promoters on catalyst performance – can only be explained invoking the amount of carbonaceous deposits on the catalysts surface when the difference in the magnitude of coking is sizable. With this in mind, caution should be taken when interpreting thermogravimetric data such as that in Figure 5 bottom right, which shows the TGA plots of catalysts spent in the continuous deoxygenation of triolein. Indeed, while 20% Ni-5% Cu/Al₂O₃ exhibited less coking and better activity than 20% Ni/Al₂O₃, the difference in their associated carbonaceous deposits is too small (<1%) to be significant. The fact that the weight losses of spent catalysts from fixed bed experiments were almost negligible is in itself noteworthy, particularly since an unsaturated feed was employed in an effort to exacerbate catalyst coking and deactivation.

In short, although longer and/or more stringent experiments may be necessary to accentuate coking and thereby uncover the role of promoters in retarding catalyst deactivation arising from accumulated carbonaceous deposits, the present work shows that Ni-Cu deCO_x catalysts have the potential to outperform Ni-only formulations and that in some instances this enhancement can be attributed to the ability of Cu to suppress cracking and coke-induced deactivation, the capacity of Cu addition to curb coking in Ni-based deoxygenation catalysts being consistent with a recent report by Guo et al. [39]. It should be appreciated that these results were acquired using lipid feeds for which the dilution level is far from representative of industrial conditions. Therefore, a future contribution will focus on the use of concentrated waste lipid feeds.

4. Conclusions

Semi-batch studies indicate that Cu is a very effective promoter of Ni for the deCO_x of tristearin at 260 °C, tristearin conversion increasing from 27% over 20% Ni/Al₂O₃ to 97% over 20% Ni-5% Cu/Al₂O₃. At 350 °C, Sn is also a promising promoter, increasing selectivity to C17

from 21% over 20% Ni/Al₂O₃ to 56% over 20% Ni-1% Sn/Al₂O₃. Cu also promoted the deoxygenation of stearic acid in semi-batch mode, 20% Ni-5% Cu/Al₂O₃ exhibiting higher stearic acid conversion than 20% Ni/Al₂O₃ at both 260 and 300 °C, as well as considerably higher selectivity to diesel-like hydrocarbons at the higher reaction temperature. The benefit of promoting 20% Ni/Al₂O₃ with 5% Cu was confirmed in fixed bed experiments with a triolein feed, for which the Ni-Cu bimetallic catalyst exhibited higher selectivity to long chain hydrocarbons than the Ni-only catalyst, particularly at the beginning of the reaction.

Improvements in deCO_x performance arising from Cu or Sn addition to Ni catalysts does not appear related to particle size effects. Copper promotion arises from a combination of factors including the destabilization of NiO and the consequent increase in the proportion of surface Ni⁰, which is believed the catalytically active phase for lipid deoxygenation. Thermogravimetric analysis of spent catalysts suggests that Cu promotion may also be ascribed to the suppression of surface coking and hence catalyst deactivation, albeit only when there are significant differences in the amount of carbonaceous deposits between distinct catalysts. This enhanced resistance to coke-induced deactivation may reflect the ability of Cu to curb the cracking activity of Ni-only catalysts and impart superior selectivity to long chain hydrocarbons via both geometric and electronic effects.

Acknowledgements

This work was supported in part by the National Science Foundation (NSF) under Grant No. 1437604, by the U.S. Department of Energy (DOE) under award DE-FG36-08GO88043 and by a Seed Grant from the University of Kentucky Center for Applied Energy Research. Funding from the British Council under the Global Innovation Initiative for the GB3-Net project is also gratefully acknowledged. Any opinions, findings, conclusions or recommendations expressed herein are those of the authors and do not necessarily reflect the views of the Department of Energy. Research materials produced in the course of this work, including samples comprising reaction products as well as physical and digital data arising from the characterization and analysis of catalysts and reaction products, will be kept and remain accessible until 2020.

References

1. J. Fargoine, J. Hill, D. Tilman, S. Polasky, P. Hawthorne, *Science* 319 (2008) 1235-1238.
2. D. Tilman, R. Socolow, J.A. Foley, J. Hill, E. Larson, L. Lynd, S. Pacala, J. Reilly, T. Searchinger, C. Somerville, R. Williams, *Science* 325 (2009) 270-271.
3. A.S. Berenblyum, T.A. Podoplelova, R.S. Shamsiev, E.A. Katsman, V.Y. Danyushevsky, V.R. Flid, *Catal. Ind.* 4 (2012) 209-214.
4. <http://www.uop.com/processing-solutions/renewables/green-diesel/#biodiesel> (accessed October 2015).
5. D. Ogunkoya, W.L. Roberts, T. Fang, N. Thapaliya, *Fuel* 140 (2015) 541-554.
6. B. Donnis, R.G. Egeberg, P. Blom, K.G. Knudsen, *Topics in Catalysis* 52 (2009) 229-240.
7. I. Kubicková, M. Snåre, K. Eränen, P. Mäki-Arvela, D.Y. Murzin, *Catal. Today* 106 (2005) 197-200.
8. H. Zuo, Q. Liu, T. Wang, L. Ma, Q. Zhang, Q. Zhang, *Energy Fuels* 26 (2012) 3747-3755.
9. B. Peng, X. Yuan, C. Zhao, J.A. Lercher, *Journal of the American Chemical Society* 134 (2012) 9400-9405.
10. P. Mäki-Arvela, I. Kubickova, M. Snåre, K. Eränen, D.Y. Murzin, *Energy & Fuels* 21 (2007) 30-41.
11. M. Snåre, I. Kubicková, P. Mäki-Arvela, K. Eränen, J. Wärnä, D.Y. Murzin, *Chem. Eng. J.* 134 (2007) 29-34.
12. P. Mäki-Arvela, M. Snåre, K. Eränen, J. Myllyoja, D.Y. Murzin, *Fuel* 87 (2008) 3543-3549.
13. I. Simakova, O. Simakova, P. Mäki-Arvela, D.Y. Murzin, *Catal. Today* 150 (2010) 28-31.
14. J.G. Immer, M.J. Kelly, H.H. Lamb, *Appl. Catal., A* 375 (2010) 134-139.

15. J.G. Immer, H.H. Lamb, *Energy Fuels* 24 (2010) 5291-5299.
16. E.W. Ping, J. Pierson, R. Wallace, J.T. Miller, T.F. Fuller, C.W. Jones, *Appl. Catal., A* 396 (2011) 85-90.
17. A.S. Berenblyum, V.Y. Danyushevsky, E.A. Katsman, T.A. Podoplelova, V.R. Flid, *Petroleum Chemistry* 50 (2010) 305-311.
18. A.S. Berenblyum, T.A. Podoplelova, R.S. Shamsiev, E.A. Katsman, V.Y. Danyushevsky, *Petroleum Chemistry* 51 (2011) 336-341.
19. P.T. Do, M. Chiappero, L.L. Lobban, D.E. Resasco, *Catalysis Letters* 130 (2009) 9-18.
20. M. Chiappero, P.T.M. Do, S. Crossley, L.L. Lobban, D.E. Resasco, *Fuel* 90 (2011) 1155-1165.
21. J.-G. Na, B.E. Yi, J.K. Han, Y.-K. Oh, J.-H. Park, T.S. Jung, S.S. Han, H.C. Yoon, J.-N. Kim, H. Lee, C.H. Ko, *Energy* 47 (2012) 25-30.
22. T. Morgan, D. Grubb, E. Santillan-Jimenez, M. Crocker, *Top. Catal.* 53 (2010) 820-829.
23. E. Santillan-Jimenez, T. Morgan, J. Lacny, S. Mohapatra, M. Crocker, *Fuel* 103 (2013) 1010-1017.
24. C. Kordulis, K. Bourikas, M. Gousi, E. Kordouli, A. Lycourghiotis, *Appl. Catal., B* 181 (2016) 156-196.
25. T. Morgan, E. Santillan-Jimenez, A.E. Harman-Ware, Y. Ji, D. Grubb, M. Crocker, *Chemical Engineering Journal* 189-190 (2012) 346-355.
26. E. Santillan-Jimenez, T. Morgan, J. Shoup, A.E. Harman-Ware, M. Crocker, *Catalysis Today* (2013).
27. E. Santillan-Jimenez, M. Crocker, *Journal of Chemical Technology & Biotechnology* 87 (2012) 1041-1050.

28. J.P. Ford, J.G. Immer, H.H. Lamb, *Topics in Catalysis* 55 (2012) 175-184.
29. M. Snåre, I. Kubicková, P. Mäki-Arvela, D. Chichova, K. Eränen, D.Y. Murzin, *Fuel* 87 (2008) 933-945.
30. H. Bernas, K. Eränen, I. Simakova, A.-R. Leino, K. Kordás, J. Myllyoja, P. Mäki-Arvela, T. Salmi, D.Y. Murzin, *Fuel* 89 (2010) 2033-2039.
31. S. Lestari, P. Mäki-Arvela, H. Bernas, O. Simakova, R. Sjöholm, J. Beltramini, G.Q. Lu, J. Myllyoja, I. Simakova, D.Y. Murzin, *Energy & Fuels* 23 (2009) 3842-3845.
32. P.i. Mäki-Arvela, B. Rozmysłowicz, S. Lestari, O. Simakova, K. Eränen, T. Salmi, D.Y. Murzin, *Energy & Fuels* 25 (2011) 2815-2825.
33. E. Santillan-Jimenez, T. Morgan, J. Shoup, A. Harman-Ware, M. Crocker, *Catal. Today* 237 (2014) 136-144.
34. J.C. Serrano-Ruiz, J.A. Dumesic, *Energy Environ. Sci.* 4 (2011) 83-99.
35. J.A. Botas, D.P. Serrano, A. García, J. De Vicente, R. Ramos, *Catal. Today* 195 (2012) 59-70.
36. N. Galea, D. Knapp, T. Ziegler, *Journal of Catalysis* 247 (2007) 20-33.
37. V. Fierro, O. Akdim, C. Mirodatos, *Green Chemistry* 5 (2003) 20-24.
38. A.G. Boudjahem, M. Chettibi, S. Monteverdi, M. M. Bettabar, *Journal of Nanoscience and Nanotechnology* 9 (2009) 3546-3554.
39. Q. Guo, M. Wu, K. Wang, L. Zhang, X. Xu, *Ind. Eng. Chem. Res.* 54 (2015) 890-899.
40. P.C.M. Van Stiphout, D.E. Stobbe, F.T. V.D. Scheur, J.W. Geus, *Appl. Catal.* 40 (1988) 219-246.
41. V.A. Yakovlev, S.A. Khromova, O.V. Sherstyuk, V.O. Dundich, D.Y. Ermakov, V.M. Novopashina, M.Y. Lebedev, O. Bulavchenko, V.N. Parmon, *Catal. Today* 144 (2009) 362-366.

42. E. Nikolla, J. Schwank, S. Linic, *J. Catal.* 263 (2009) 220-227.
43. E. Nikolla, A. Holewinski, J. Schwank, S. Linic, *Journal of American Chemical Society* 128 (2006) 11354-11355.
44. R.W. Gosselink, S.A.W. Hollak, S.-W. Chang, J.v. Haveren, K.P.d. Jong, D.S.v. Es, *ChemSusChem* 6 (2013) 1576-1597.
45. E. Santillan-Jimenez, T. Morgan, R. Loe, M. Crocker, *Catal. Today* 258 (2015) 284-293.
46. E.G. Bligh, W.J. Dyer, *Canadian Journal of Biochemistry and Physiology* 37 (1959) 911-917.
47. M.H. Wilson, J. Groppo, A. Placido, S. Graham, S.A. Morton, III, E. Santillan-Jimenez, A. Shea, M. Crocker, C. Crofcheck, R. Andrews, *Appl. Petrochem. Res.* 4 (2014) 41-53.
48. T. Morgan, E. Santillan-Jimenez, M. Crocker, *Energy & Fuels* 28 (2014) 2654-2662.
49. A. Vizcaíno, A. Carrero, J. Calles, *Int. J. Hydrogen Energy* 32 (2007) 1450-1461.
50. A. Carrero, J. Calles, A. Vizcaíno, *Appl. Catal., A* 327 (2007) 82-94.
51. J.-H. Lee, E.-G. Lee, O.-S. Joo, K.-D. Jung, *Appl. Catal., A* 269 (2004) 1-6.
52. J.M. Rynkowski, T. Paryjczak, M. Lenik, *Appl. Catal., A* 106 (1993) 73-82.
53. B.C. Miranda, R.J. Chimentão, J. Szanyi, A.H. Braga, J.B.O. Santos, F. Gispert-Guirado, J. Llorca, F. Medina, *Appl. Catal., B* 166–167 (2015) 166-180.
54. Y. Li, J. Chen, L. Chang, Y. Qin, *J. Catal.* 178 (1998) 76-83.
55. J. Zieliński, *J. Catal.* 76 (1982) 157-163.
56. P. Castaño, B. Pawelec, J.L.G. Fierro, J.M. Arandes, J. Bilbao, *Fuel* 86 (2007) 2262-2274.
57. X. Zhu, Y.-p. Zhang, C.-j. Liu, *Catalysis Letters* 118 (2007) 306-312.

58. M. Mihaylov, O. Lagunov, E. Ivanova, K. Hadjiivanov, *Topics in Catalysis* 54 (2011) 308-317.
59. A. Kitla, O.V. Safonova, K. Föttinger, *Catal Letters* 143 (2013) 517-530.
60. M.K. Neylon, S. Choi, H. Kwon, K.E. Curry, L.T. Thompson, *Appl. Catal., A* 183 (1999) 253-263.
61. E. Laperdrix, I. Justin, G. Costentin, O. Saur, J.C. Lavalley, A. Aboulayt, J.L. Ray, C. Nédéz, *Appl. Catal., B* 17 (1998) 167-173.
62. M. Snåre, I. Kubičková, P. Mäki-Arvela, K. Eränen, D.Y. Murzin, *Ind. Eng. Chem. Res.* 45 (2006) 5708-5715.
63. T. Ito, Y. Sakurai, Y. Kakuta, M. Sugano, K. Hirano, *Fuel Process. Technol.* 94 (2012) 47-52.
64. A.S. Berenblyum, R.S. Shamsiev, T.A. Podoplelova, V.Y. Danyushevsky, *Russ. J. Phys. Chem.* 86 (2012) 1199-1203.
65. A.S. Berenblyum, V.Y. Danyushevsky, E.A. Katsman, R.S. Shamsiev, V.R. Flid, *Pet. Chem.* 53 (2013) 362-366.
66. N. Mahata, V. Vishwanathan, *J. Catal.* 196 (2000) 262-270.
67. J.M. Parera, N.S. Figoli, E.L. Jablonski, M.R. Sad, J.N. Beltramini, *Stud. Surf. Sci. Catal.* 6 (1980) 571-576.
68. S. Harnos, G. Onyestyák, D. Kalló, *React. Kinet., Mech. Catal.* 106 (2012) 99-111.
69. B. Rozmysłowicz, P. Mäki-Arvela, A. Tokarev, A.-R. Leino, K. Eränen, D.Y. Murzin, *Industrial & Engineering Chemistry Research* 51 (2012) 8922-8927.
70. B. Peng, C. Zhao, S. Kasakov, S. Foraita, J.A. Lercher, *Chemistry* 19 (2013) 4732-4741.
71. P. Song, D. Wen, Z.X. Guo, T. Korakianitis, *PCCP* 10 (2008) 5057-5065.

Figure captions

Figure 1. H₂ TPR profiles of the fresh catalysts.

Figure 2. Reaction scheme for stearic acid deoxygenation (after refs. [65,66]).

Figure 3. Boiling point distribution plots of the feed and the liquid products obtained from triolein deoxygenation in fixed bed mode at 260 °C and 580 psi over 20% Ni/Al₂O₃ (left), and 20% Ni-5% Cu/Al₂O₃ (right).

Figure 4. Boiling point distribution plots of the feed and the liquid products obtained from algal lipids deoxygenation in fixed bed mode at 260 °C and 580 psi over 20% Ni/Al₂O₃ (left), and 20% Ni-5% Cu/Al₂O₃ (right).

Figure 5. TGA profiles of catalysts spent upgrading tristearin at 260°C for 6 h in a semibatch reactor (top left), tristearin at 350°C for 6 h in a semibatch reactor (top right), stearic acid at 300 °C for 1.5 h in a semibatch reactor (bottom left), and triolein at 260 °C for 4 h in a fixed bed reactor (bottom right).

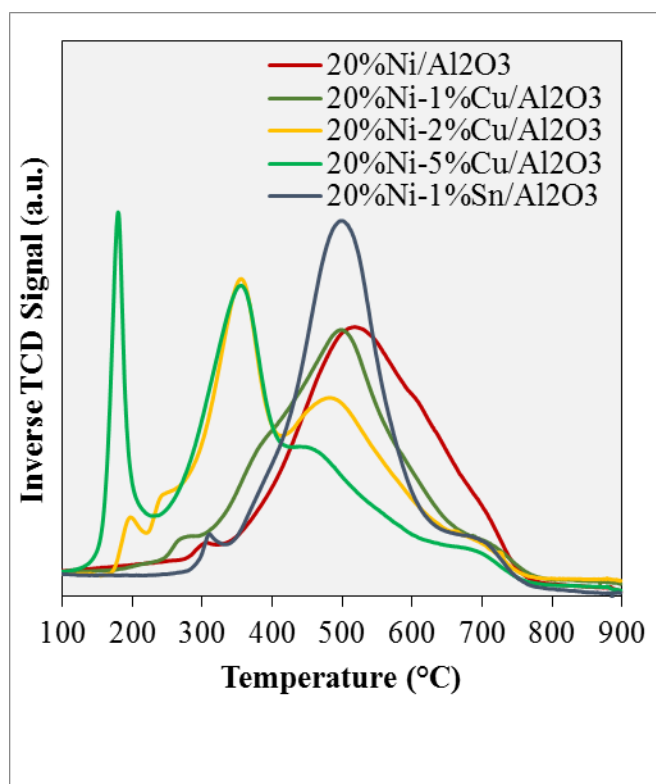


Fig. 1

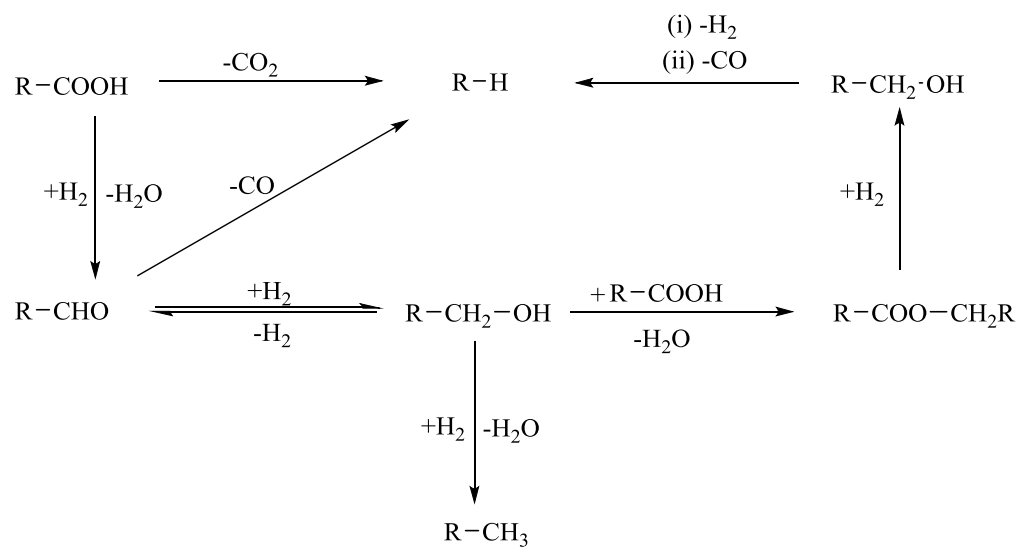


Fig. 2

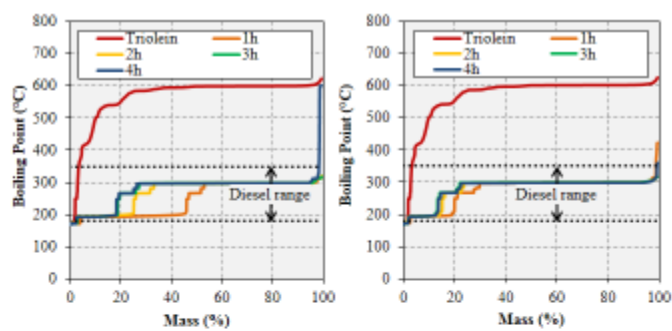


Fig. 3

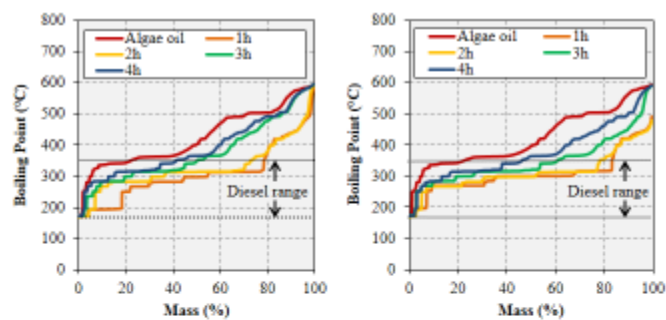


Fig. 4

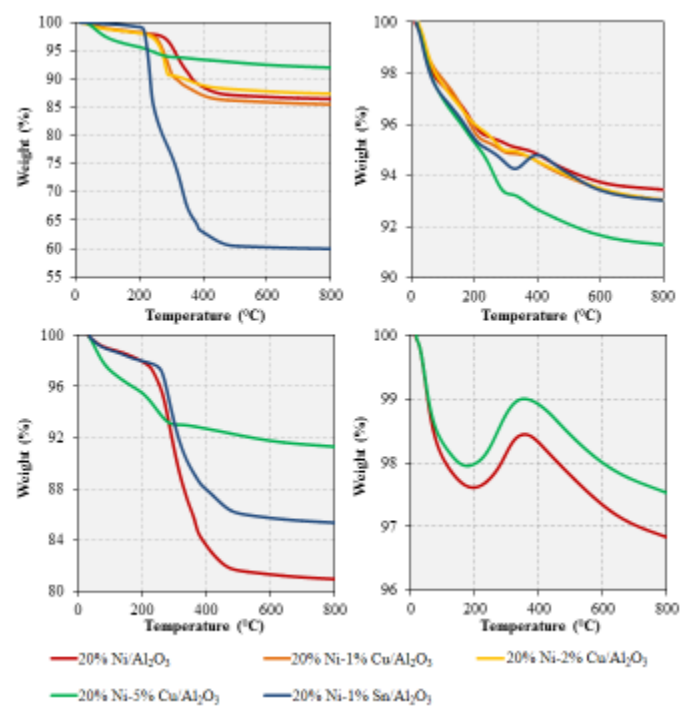


Fig. 5

Table 1. Textural properties and metal dispersion of the catalysts studied.

Catalyst	BET surface area (m²/g)	Pore volume (cm³/g)	Avg. pore diameter (nm)	Avg. NiO particle size (nm)*
20% Ni/Al ₂ O ₃	134	0.30	9.0	7.4
20% Ni-1% Cu/Al ₂ O ₃	148	0.32	8.7	7.7
20% Ni-2% Cu/Al ₂ O ₃	137	0.30	8.8	6.4
20% Ni-5% Cu/Al ₂ O ₃	129	0.28	8.8	10.7
20% Ni-1% Sn/Al ₂ O ₃	141	0.46	8.9	6.5

*As measured from the powder X-ray diffractograms of the catalysts calcined under static air for 3 h at 500 °C.

Table 2. Semi-batch mode deoxygenation of tristearin over alumina-supported Ni-based catalysts (580 psi of H₂, 6 h reaction time).*

Catalyst	Reaction Temperature (°C)	Conversion (%) ^a	Selectivity to [Yield of] C10-C17 (%) ^{b, d}	Selectivity to [Yield of] C17 (%) ^{c, d}
20% Ni/Al ₂ O ₃	260	27	87 [23]	63 [17]
20% Ni-1% Cu/Al ₂ O ₃	260	27	89 [24]	56 [15]
20% Ni-2% Cu/Al ₂ O ₃	260	85	95 [81]	65 [55]
20% Ni-5% Cu/Al ₂ O ₃	260	97	99 [96]	71 [69]
20% Ni-1% Sn/Al ₂ O ₃	260	11	8 [1]	3 [1]
20% Ni/Al ₂ O ₃	300	98	97 [95]	53 [52]
20% Ni-1% Cu/Al ₂ O ₃	300	>99	>99 [98]	54 [53]
20% Ni-2% Cu/Al ₂ O ₃	300	98	98 [96]	55 [54]
20% Ni-5% Cu/Al ₂ O ₃	300	>99	>99 [98]	62 [61]
20% Ni-1% Sn/Al ₂ O ₃	300	38	45 [17]	27 [10]
20% Ni/Al ₂ O ₃	350	>99	88 [87]	21 [21]
20% Ni-1% Cu/Al ₂ O ₃	350	>99	86 [85]	15 [15]
20% Ni-2% Cu/Al ₂ O ₃	350	>99	81 [80]	3 [3]
20% Ni-5% Cu/Al ₂ O ₃	350	>99	98 [97]	49 [49]
20% Ni-1% Sn/Al ₂ O ₃	350	>99	97 [96]	56 [55]

*All experiments for which results are shown were performed a minimum of two times, average standard deviations being 3.1, 3.6, and 9.1% for conversion, selectivity to C10-C17, and selectivity to C17, respectively.

^a Conversion = wt% of product with bp < 375°C.

^b Selectivity to C10-C17 = $100 \times [(\text{wt\% of product with bp} < 314^\circ\text{C} - \text{wt\% of product with bp} < 177^\circ\text{C}) / (\text{wt\% of product with bp} < 375^\circ\text{C})]$.

^c Selectivity to C17 = $100 \times [(\text{wt\% of product with bp} < 314^\circ\text{C} - \text{wt\% of product with bp} < 295^\circ\text{C}) / (\text{wt\% of product with bp} < 375^\circ\text{C})]$.

^d The corresponding yield (conversion \times selectivity) values are shown between brackets.

Table 3. Semi-batch mode deoxygenation of stearic acid over alumina-supported Ni-based catalysts (300 psi of H₂, 1.5 h reaction time).*

Catalyst	Reaction Temperature (°C)	Conversion (%) ^a	Selectivity to [Yield of] C10-C17 (%) ^{b, d}	Selectivity to [Yield of] C17 (%) ^{c, d}
20% Ni/Al ₂ O ₃	260	39	15 [6]	2 [1]
20% Ni-5% Cu/Al ₂ O ₃	260	54	13 [7]	7 [4]
20% Ni-1% Sn/Al ₂ O ₃	260	30	7 [2]	3 [1]
20% Ni/Al ₂ O ₃	300	92	76 [70]	66 [61]
20% Ni-5% Cu/Al ₂ O ₃	300	98	86 [84]	79 [77]
20% Ni-1% Sn/Al ₂ O ₃	300	39	23 [9]	17 [7]

*All experiments for which results are shown were performed a minimum of two times, average standard deviations being 7.3, 11.9, and 9.1% for conversion, selectivity to C10-C17, and selectivity to C17, respectively.

^a Conversion = 100 – (wt% of product with bp < 375°C – wt% of product with bp < 350°C).

^b Selectivity to C10-C17 = 100 × <(wt% of product with bp < 314°C – wt% of product with bp < 177°C)/[100 - (wt% of product with bp < 375°C – wt% of product with bp < 350°C)]>.

^c Selectivity to C17 = 100 × <[(wt% of product with bp < 314°C – wt% of product with bp < 295°C)/ [100 - (wt% of product with bp < 375°C – wt% of product with bp < 350°C)]>.

^d The corresponding yield (conversion × selectivity) values are shown between brackets.